Journal of
Materials Chemistry B

Accepted Manuscript

This article can be cited before page numbers have been issued, to do this please use: Y. Zhou , Q. Zhang, J. Wu, C. Xi and M. E. Meyerhoff, *J. Mater. Chem. B*, 2018, DOI: 10.1039/C8TB01814F.

ROYAL SOCIETY OF CHEMISTRY

rsc.li/materials-b

View Article Online
DOI: 10.1039/C8TB01814F

Journal Name

ARTICLE

Synthesis and Characterization of a Fluorinated *S*-Nitrosothiol as the Nitric Oxide Donor for Fluoropolymer-Based Biomedical Device Applications

Received 00th January 20xx,
Accepted 00th January 20xx

DOI: 10.1039/x0xx00000x

www.rsc.org/

Yang Zhou,[a] Qi Zhang,[a] Jianfeng Wu,[b] Chuanwu Xi[b] and Mark E. Meyerhoff*[a]

Fluorinated polymers are widely used as biomaterials in various biomedical implant and device applications. However, thrombogenicity, surface-induced inflammation, and risk of microbial infection remain key issues that can limit their use. In this work, we describe the first nitric oxide (NO) releasing fluorinated polymer, in which a new fluorinated NO donor, *S*-nitroso-*N*-pentafluoropropionylpenicillamine (C_2F_5-SNAP), is incorporated within the polyvinylidene fluoride (PVDF) tubing. The synthesis, decomposition kinetics, and NO-release characteristics of the C_2F_5-SNAP species are described in detail. Then, using a simple solvent swelling method, we demonstrate that C_2F_5-SNAP can readily be doped into PVDF tubing. The resulting tubing can release NO for 11 days under physiological conditions, with an NO flux > 0.5×10^{-10} mol/cm^2·min over the first 7 days. Due to fluorous-fluorous interactions, the leaching of the fluorinated NO donor and its decomposed products is shown to be very low (less than 5 nmol/mg, total). Further, the new NO-releasing PVDF tubing exhibits significant antimicrobial activity (compared to undoped PVDF tubing) against both gram positive and negative *S. aureus* and *P. aeruginosa* bacterial strains over a 7 d test period. This new NO-releasing fluorinated polymer is likely to have the potential to improve the biocompatibility and antimicrobial activity of various biomedical devices.

Introduction

Fluorinated polymers have attracted significant attention for use in various biomedical implants/devices since polytetrafluoroethylene (PTFE) was first discovered in 1983.[1-5] This class of polymers can be divided into two general categories based on their corresponding components; perfluorinated and partially fluorinated polymers.[6] With fluorinated groups in the polymer backbone, fluorinated polymers have distinct characteristics, including high thermal stability, excellent chemical resistance, low coefficient of friction, high tensile strength, enhanced biocompatibility and interesting electrical properties.[6] The use of fluorinated polymers in blood contacting biomedical applications have a long history because of these distinct properties.[2] Currently, the perfluorinated polymer expanded PTFE, and the partially fluorinated polymer polyvinylidene fluoride (PVDF), are the two commercial fluorinated polymers most widely used to prepare biomedical implants and devices. For example, a variety of medical materials/devices, such as vascular grafts, cardiovascular patches, sutures and stents, are made of expanded PTFE material.[2] PVDF polymers are commonly employed in suture materials and surgical meshes.[1] In addition, a fluorosiloxane hydrogel (Lotrafilcon A) is commercially available for use in the contact lens market.[7]

It is known that fluorinated polymers have much better biocompatibility compared to corresponding non-fluorinated polymers.[5] In particular, fluorinated polymers have been reported to offer both lower thrombogenicity and decreased inflammatory response.[5] Multiple studies provide direct evidence that fluorinated polymers can reduce platelet adhesion and activation.[5] For instance, copolymers of PVDF and hexafluoropropylene (HFP) exhibited low platelet reactivity and better blood compatibility than more conventional non-fluorinated polymers.[8] The biocompatibility of non-fluorinated polymers can also be greatly increased through the blending or surface fluorination with fluorinated polymers.[9-20] Additionally, the biomedical application of both fluorinated polymers and fluorinated surface-modifying polymers can decrease inflammatory response, resulting from their highly hydrophobic surface property.[21] So far, many studies have reported this antimicrobial activity through surface coating and/or doping of fluorinated polymers.[22-25]

Although fluorinated polymers offer great potential for both suppression of blood clots and reduction of bacterial adhesion and proliferation, surface-induced thrombus formation and inflammatory responses can still be triggered by such materials, and further research is needed to address those issues.[5] For example, in two separate studies, visible adhered blood clotting was observed on a PTFE surface over a relatively short time.[20, 26] Fluorinated

[a] Department of Chemistry, University of Michigan, Ann Arbor, MI 48109, USA. E-mail: mmeyerho@umich.edu
[b] Department of Environmental Health Sciences, University of Michigan School of Public Health, Ann Arbor, MI 48109, USA

† Electronic Supplementary Information (ESI) available: [details of any supplementary information available should be included here]. See DOI: 10.1039/x0xx00000x

View Article Online
DOI: 10.1039/C8TB01814F

polyethylene was also found to stimulate thrombus formation.[27] PVDF-HFP copolymers were also reported to elicit acute thrombotic responses.[28] In the practical application of PTFE catheters as insulin infusion cannulas, the lifetime of these PTFE cannulas is about ~ 3 d due to the inflammatory response and also increased risk of microbial colonization at the infusion site.[29-31] To solve the thrombus formation or inflammatory response from fluorinated polymers, only a limited number of approaches were proposed using surface modifications with bioactive molecules. For instance, expanded PTFE with surface coating of heparin provided a more thromboresistant blood contacting surface, which can greatly improve the vascular graft performance.[32] A gendine-coated PTFE tubing was proposed as an insulin infusion cannula, to show enhanced antimicrobial efficiency towards several pathogens.[29] The surface modifications of PVDF film and membrane using a peptide-click-poly(glycidylmethacrylate) polymer and a polymethacrylamide-ammoniumbetaine copolymer also was found to exhibit greater biocompatibility than the non-treated PVDF polymer.[33, 34] However, these surface modification methods are relatively complex, requiring multiple handling steps. In addition, surface-grafted molecules carry the risk of potential toxicity.

Nitric oxide (NO), an endogenously gaseous signaling molecule produced by oxidation of $_L$-arginine by a family of NO synthase enzymes,[35] has been well studied and understood for its broad and specific biofunctionalities,[35-37] including blood vasodilation, anti-platelet activity, inhibition of bacterial growth, immune modulation, anticancer activity, and biological process regulation. The NO flux released by an endothelial layer of the inner wall of blood vessels is estimated to be between 0.5 and 4.0 × 10^{-10} mol·cm^{-2}·min^{-1}.[38] However, molecular NO is highly reactive under physiological conditions, and has a reported intravascular half-life of ~ 2 s.[39] In chemical and biochemical studies, various precursor molecules of NO (NO donors) have been utilized for NO release *in situ*,[40] such as *S*-nitrosothiols, *N*-diazeniumdiolates, metal nitrosyls, *N*-nitrosamines, organic nitrates and nitrites. Similar NO donors have also been widely used as promising therapeutic agents.[41-44] In particular, due to the potent antimicrobial and antithrombotic properties of NO, such NO-releasing platforms have served as a promising approach to improve the biocompatibility of medical devices.[38, 45-49] Such NO donors can be chemically synthesized as part of the polymers (covalently attached) or doped into medical-grade polymers. NO is then released from the surface of these parent polymers when the polymer is in contact with water/blood or other physiological fluid, to mimic the NO generated from physiological endothelial layers.

Due to the potential antimicrobial and antithrombotic functionalities of NO, the development of novel NO-releasing polymers has received considerable attention over the last decade.[38, 46, 50] Recent work from our laboratory has demonstrated the increased biocompatibility and antimicrobial activity of many medical-grade polymers including poly(lactic-co-glycolic acid), Elast-eon E2As, CarboSil polymer, silicone rubber, and polyurethane,[51-61] *via* the incorporation of a nitrosothiol (e.g. *S*-nitroso-*N*-acetyl-penicillamine, SNAP, in Figure 1) or *N*-diazeniumdiolates as the NO donors.[51-61] In addition, the Handa group also recently proposed the potential biomaterial applications of NO releasing polymers including silicone rubber,[62, 63] CarboSil,[64-67] and Elast-eon E2As.[68, 69] Reynolds and coworkers reported NO-releasing Tygon and polyphosphazene-based coating materials for biomedical applications.[70-72] The Schoenfisch group investigated polyurethane fibers and silicone elastomers NO-releasing silica materials.[73, 74] Frost et al. also proposed poly(L-lactic acid) film within a cyclam-based SNAP, releasing physiological levels of NO for up to 3 months.[75] Moreover, diazeniumdiolate coatings tethered on poly(ethylene terephthalate) and silicone elastomers showed antibacterial efficacy toward *Pseudomonas aeruginosa* (*P. aeruginosa*) bacteria.[76] Diazeniumdiolate-based acrylonitrile-co-1-vinylimidazole copolymers were reported to be used in sutures.[77] A diazeniumdiolate-based poly(diol citrate) elastomer was also proposed by Ameer group as a coating film for expanded PTFE vascular grafts,[78] in which NO release can only last for 2 days. These reports demonstrate that NO-releasing non-fluoropolymers have been extensively studied for potential applications in biomaterials. However, fluoropolymers with NO-release properties have not yet been reported. Therefore, it would be of great interest to explore the application of NO-releasing fluoropolymers for preparation of medical devices.

In fact, based on the basic solubility principle of like dissolves like, traditional hydrocarbon type NO donors are difficult to be incorporated into fluorinated polymers because of the higher polarity of hydrocarbons in comparison to fluorocarbons. Therefore, we hypothesize that it should be possible to impregnate a synthetically fluorinated NO donor into fluoropolymers using the simple solvent-swelling method. In addition, fluorous-fluorous interactions are widely present in the fluorinated materials, which have already been used in new affinity chromatography and enzyme immobilization technologies.[79-82] Due to the specific fluorous-fluorous interaction between pentafluoropropionyl group (C_2F_5) and the fluoro-backbone in PVDF, we also expect a decrease in leaching of chemicals from any fluorinated NO donor possessing the C_2F_5 group when doped into fluoropolymers. Therefore, in this work, we report the first NO-releasing fluorinated polymer *via* the incorporation of a novel fluorinated SNAP derivative (*S*-nitroso-*N*-pentafluoropropionylpenicillamine, C_2F_5-SNAP, see Fig. 1) into a PVDF polymer. The method used to synthesize C_2F_5-SNAP is described, and its stability is investigated by measuring its decomposition kinetics. In addition, the decomposition products derived from C_2F_5-SNAP are characterized. The synthetic C_2F_5-SNAP NO donor is then successfully impregnated into PVDF tubing *via* a solvent swelling approach using tetrahydrofuran (THF) as the swelling solvent. The NO-release profiles are evaluated from C_2F_5-SNAP-doped PVDF tubing under physiological conditions. Finally, the new NO-releasing PVDF tubing is also investigated for its antimicrobial activity during 7 d of incubation with two bacterial strains, *S. aureus* and *P. aeruginosa*.

View Article Online
DOI: 10.1039/C8TB01814F
Journal Name ARTICLE

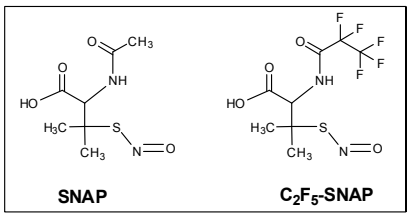

Fig. 1 The chemical structures of SNAP and C_2F_5-SNAP NO donors.

Results and discussion

Synthesis and stability test of C_2F_5-SNAP

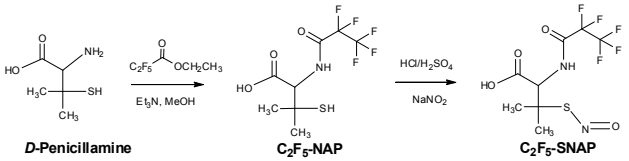

Scheme 1. Synthesis of C_2F_5-SNAP NO donor.

In our previous studies regarding the synthesis of non-fluorinated SNAP derivatives as NO donors, we found that the modification of the free carboxylic acid group of SNAP with amine functional groups (to form amides) decreased both the thermal and the photochemical stability of the desired NO donor.[83] In addition, tertiary *S*-nitrosothiols are known to be relatively thermally stable, but very photochemically unstable.[83] Furthermore, either the substitution or the incorporation of fluorine functional groups into the gem-dimethyl groups in the SNAP structure would likely cause further instability of the resulting NO donors due to the strong electron-withdrawing effect from these fluorine functional groups. Therefore, our goal was to retain the free carboxylic acid group, the tertiary structure of the nitrosothiol, and the gem-dimethyl groups in our design of any fluorinated derivative of SNAP. The acetyl group was finally selected as the site of interest for incorporation of the fluorine atoms. The novel fluorinated SNAP derivative (C_2F_5-SNAP) was therefore selected as the target species (Figure 1). The synthesis of C_2F_5-SNAP was completed *via* two sequential reaction steps from commercial *D*-penicillamine in Scheme 1. This two-step gram-scale synthesis proceeded without incident with ~ 84% overall yield. In the first step, the nucleophile, *D*-penicillamine, is readily attacked at the carbonyl group at the corresponding fluorinated ester,[84] which is followed by a subsequent elimination of ethanol. The presence of triethylamine plays a critical role in neutralizing the free carboxylic acid in *D*-penicillamine. In the absence of triethylamine, the reaction does not occur. The presence of free carboxylic acid might potentially prevent the elimination step following the completion of the nucleophilic addition reaction. The resulting free thiol, C_2F_5-NAP, was used directly in the next step. As expected, the nitrosylation of C_2F_5-NAP can be easily completed using the classical SNAP synthetic method with nitrous acid.[85] Interestingly, the desired product was able to be extracted by dichloromethane during the workup, indicating that the polarity of C_2F_5-SNAP is greatly decreased due to the presence of the fluorinated functional group. Target C_2F_5-SNAP was obtained as a greenish oil, which had the characteristic color of SNAP.

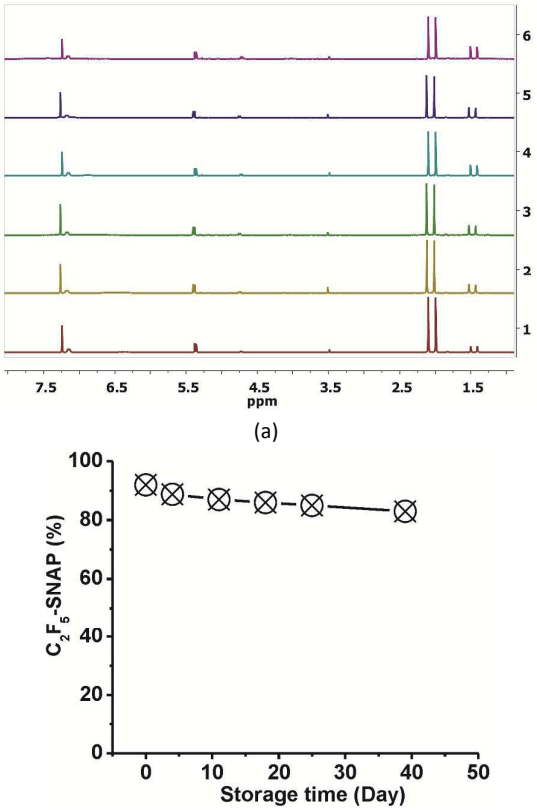

Fig. 2 (a) ^{1}H NMR spectra for the thermal stability of C_2F_5-SNAP oil (CH: ~ 5.39 ppm; CH_3: 2.12 and 2.01 ppm) at - 20 ^{o}C under argon and dark conditions after (1) day 0, (2) day 4, (3) day 11, (4) day 18, (5) day 25, and (6) day 39; (b) C_2F_5-SNAP remained percentage vs. storage time at - 20 ^{o}C under argon and dark conditions.

S-Nitrosothiols have been reported to be quite unstable under both photochemical and thermal conditions.[86, 87] With the presence of a perfluoroalkyl chain (CF_3CF_2) in C_2F_5-SNAP, it is very important to evaluate its stability due to the fluorinated functional group having a strong electron withdrawing ability. Under vacuum conditions at room temperature (23 ^{o}C) for 18 h, C_2F_5-SNAP decomposed ~ 5%. The stability of C_2F_5-SNAP stored in a freezer at - 20 ^{o}C was examined by ^{1}H NMR spectroscopy. The fluorinated SNAP derivative was found to be slightly decomposed at -20 ^{o}C under argon and dark conditions (see Fig. 2a) based on ^{1}H NMR spectroscopy data. After being stored in the freezer for 39 d, ~ 83% of C_2F_5-SNAP remained (Fig. 2b). In addition, C_2F_5-SNAP decomposed ~ 15% in a refrigerator set at 1 ^{o}C over 7 d under dark conditions (data not shown). These results suggest that C_2F_5-SNAP is thermally unstable in its oil phase due to the presence of the CF_3CF_2 group. In contrast, SNAP is very stable at -20 ^{o}C in the freezer, with no decomposition observed over several years. The results above suggest that the presence of the C_2F_5 group causes a decrease in the observed thermal stability of the new C_2F_5-SNAP species.

View Article Online
DOI: 10.1039/C8TB01814F

Decomposition kinetics of C_2F_5-SNAP

To further evaluate the stability of C_2F_5-SNAP as an NO donor, kinetic studies of its photochemical and thermal decomposition were carried out using UV/Vis spectroscopy. Steady-state photolysis of C_2F_5-SNAP (~ 206.0 μM) at 23 °C in a mixture of PBS and DMSO (50:50, v/v) was carried out using as described in the experimental section (see above). UV/Vis spectra of the photodecomposition of C_2F_5-SNAP are shown in Figure 3. The absorbance at 341 nm is the characteristic UV-Vis band of the $n_O \rightarrow \pi^*$ transition, which was observed to continuously decrease and finally flatten. The corresponding plot of absorbance at 341 nm vs. time is shown in the Fig. 3 insert. The data were fitted to a first-order rate equation (Fig. 3 insert, line), giving an observed rate constant k_{obs} = (1.60 ± 0.10) × 10^{-2} s^{-1} and a half-life of ~ 43 s.

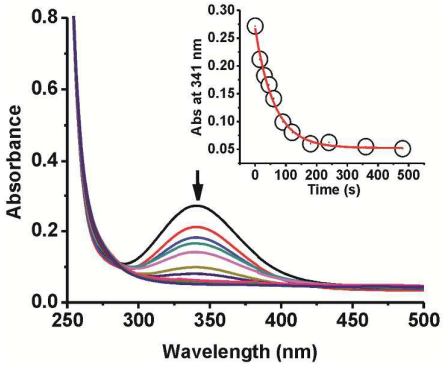

Fig. 3 UV/Vis spectra for the photolysis of C_2F_5-SNAP (~ 206.0 μM) at 23 °C in a mixture of PBS and DMSO (50:50, v/v). Inset: Plot of absorbance at 341 nm vs. time for this reaction and solid line is fit to first order rate equation line.

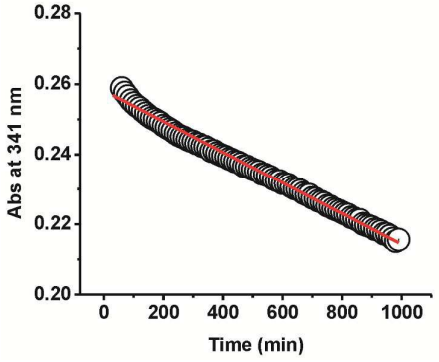

Fig. 4 Plot of absorbance at 341 nm vs. time for the thermal decomposition of C_2F_5-SNAP (~ 206.0 μM) at 37 °C in a mixture of PBS and DMSO (50:50, v/v).

The thermal decomposition of C_2F_5-SNAP (~ 206.0 μM) at 37 °C was also carried out in a mixture of PBS and DMSO (50:50, v/v). The kinetic study of this decomposition was also monitored at 341 nm (see Fig. 4). The absorbance data vs. time was fitted with a zero-order rate equation giving an observed rate constant k_{obs} of (4.39 ± 0.04) × 10^{-5} μM min^{-1}. The half-life for this thermal decomposition of C_2F_5-SNAP at 37 °C is ~ 8.08 h.

To further compare with the NO release profiles between C_2F_5-SNAP and SNAP, we also carried out the photolytic and thermal decomposition studies of SNAP in a mixture of PBS and DMSO (50:50, v/v). The corresponding kinetic data are summarized in Fig. 1S and Fig. 2S (see Supporting Information). Photolysis of SNAP (250.0 μM) was observed to be a first-order reaction with rate constant k_{obs} = (1.50 ± 0.03) × 10^{-2} s^{-1} ($t_{1/2}$ ~ 46 s). Therefore, C_2F_5-SNAP and SNAP exhibit similar lifetimes upon irradiation. Under the same thermal conditions at 37 °C, SNAP (206.0 μM) decomposes *via* a zero-order reaction (k_{obs} = (3.45 ± 0.02) × 10^{-5} μM Min^{-1}). However, the observed rate constant (k_{obs} = (3.45 ± 0.02) × 10^{-5} μM Min^{-1}) of SNAP is lower than that of C_2F_5-SNAP (k_{obs} = (4.39 ± 0.04) × 10^{-5} μM min^{-1}), indicating that C_2F_5-SNAP decomposes more rapidly than SNAP. This result also agrees with the conclusion obtained in the stability studies reported above. That is, the thermal stability of C_2F_5-SNAP is decreased compared to SNAP due to the presence of the fluorinated group.

Decomposition product analysis

The NO-generation mechanism from *S*-nitrosothiols is well characterized under thermal, light irradiation, and Cu^+ mediated reduction.[86, 88] NO generation from these species is associated with the homolysis of the S-N bond,[88] to generate NO and thiyl radicals. However, thiyl radicals are not generally observed as intermediates during the reaction, as these radicals rapidly dimerize into a disulfide final product.[88] For the new C_2F_5-SNAP species, it is of significance to quantify both the rate of NO release and the corresponding decomposition products. To determine the stoichiometry of NO release, a quantitative photolysis of C_2F_5-SNAP was conducted to quantitate the yield of NO gas generation. A solution of C_2F_5-SNAP (1.23 × 10^{-7} mol) in a mixture of PBS and DMSO (50:50, v/v) was irradiated by 350 nm lamps in a NOA reaction cell. The corresponding NO generation was analyzed by the NOA instrumentation (see Fig. 5). The total NO release from three independent photolysis experiments was determined to be 93% ± 2%.

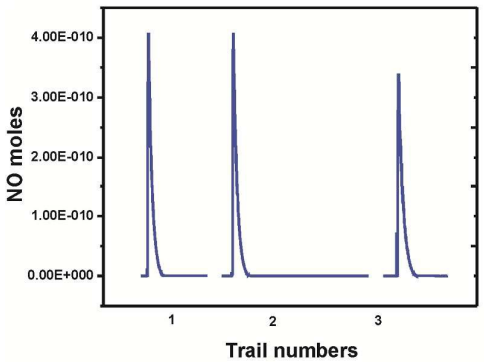

Fig. 5 NO determinations *via* NOA during photolysis of C_2F_5-SNAP (1.23 × 10^{-7} mol) in a mixture of PBS and DMSO (50:50, v/v) at room temperature.

In addition to NO, the corresponding disulfide was expected to form as a side product of the photolytic decomposition of C_2F_5-SNAP. To confirm the formation of C_2F_5-NAP disulfide, a C_2F_5-SNAP sample in $CDCl_3$ with 1% of tetramethylsilane (TMS) was analyzed by ^{1}H NMR spectroscopy before and after decomposition (see Fig.

View Article Online
DOI: 10.1039/C8TB01814F

6). Before decomposition, methide and gem-dimethyl groups within pure C_2F_5-SNAP exhibited chemical shifts at ~ 5.39, 2.12 and 2.01 ppm. After overnight thermal decomposition in the dark at room temperature, the product observed had the methide (~ 4.74 ppm) and gem-dimethyl groups (~ 1.52 and 1.43 ppm) shifted, which corresponds to the disulfide dimer of C_2F_5-NAP. Full decomposition of C_2F_5-SNAP was observed after 4 days. The identity of C_2F_5-NAP disulfide was further confirmed by HRMS results (m/z (ESI): calculated for $[M+H]^+$ 589.0519; found 589.0522). The conversion percentage to the C_2F_5-NAP disulfide was calculated to be ~ 95%, based on the presence of the internal standard TMS. This decomposed product fully agrees with the product generated during the stability testing (see Fig. 2a). These data confirm that C_2F_5-SNAP can be used as a clean NO donor, and that the disulfide dimer of C_2F_5-NAP is the only decomposition byproduct as summarized in Scheme 2.

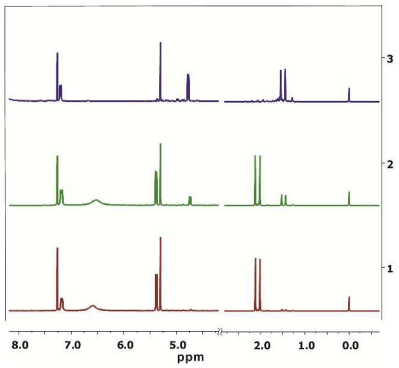

Fig. 6 ^{1}H NMR spectra for C_2F_5-SNAP before and after decomposition in $CDCl_3$ at room temperature (1) before decomposition, (2) overnight thermal decomposition, (3) completed decomposition, (C_2F_5-SNAP (CH: ~ 5.39 ppm; CH_3 : ~ 2.12 and 2.01 ppm); C_2F_5-NAP disulfide (CH: ~ 4.74 ppm; CH_3: ~ 1.52 and 1.43 ppm), CH_2Cl_2: ~ 5.30 ppm).

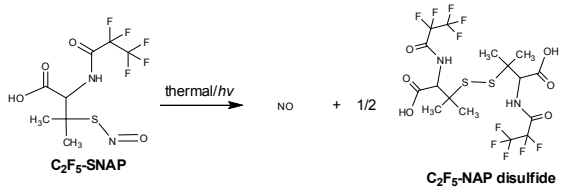

Scheme 2. NO release from C_2F_5-SNAP NO donor.

NO release from C_2F_5-SNAP doped PVDF tubing

Three PDVF tubes (1 inch in length, 1/16" ID × 1/8" OD) were swelled in a high concentration of C_2F_5-SNAP stock solution (~ 634.0 mg/mL in THF) for 24 h. After being dried under vacuum, these tubes were washed with CH_2Cl_2 (10 times) to completely remove the surface-attached chemicals. After drying under vacuum for another 24 h, the resulting PVDF tubes impregnated with C_2F_5-SNAP exhibited a dark green color characteristic of this NO donor. The corresponding NO-release profile from these PDVF tubes was recorded by an NOA instrument in PBS at 37 °C, and the results are summarized in Fig. 7. Interestingly, NO release can be observed for 11 d when the sample tubing is stored in PBS at 37 °C. The NO flux number can reach up to 10 × 10^{-10} mol/cm^2·min on the first day, but then drops to ~ 5.0 x 10^{-10} mol/cm^2·min on the second day. The NO release decreased on each succeeding day. The NO flux number observed was > 0.5 × 10^{-10} mol/cm^2·min for up to 7 d. In addition, a second swelling of PVDF tubing (1 inch in length, 1/16" ID × 1/8" OD) with a lower concentration of C_2F_5-SNAP (400.5 mg/mL in THF) demonstrated a total NO-release period of 8 d (NO-release > 0.5 × 10^{-10} mol/cm^2·min for 5 d, see Fig. 3S). Hence, by swelling the PVDF tubing with a higher concentration of C_2F_5-SNAP, NO-release time can be extended, as expected. In fact, it is not practical to quantify the total amount C_2F_5-SNAP loaded into the PVDF tubing using this solvent impregnation method, since C_2F_5-SNAP is unstable in organic phase solutions. According to the NO release determined each day by chemiluminescences measurements, the total loading of C_2F_5-SNAP in PVDF tubing was estimated to be ~ 42.3 nmol/mg. The corresponding total loading of C_2F_5-SNAP in PVDF tubing in Fig. 3S was estimated to be ~ 32.3 nmol/mg. In addition, C_2F_5-SNAP doped PVDF tubes still showed the characteristic green color after being stored < -20 °C for three months, indicating that NO-releasing tubing is stable under long-term storage in a freezer.

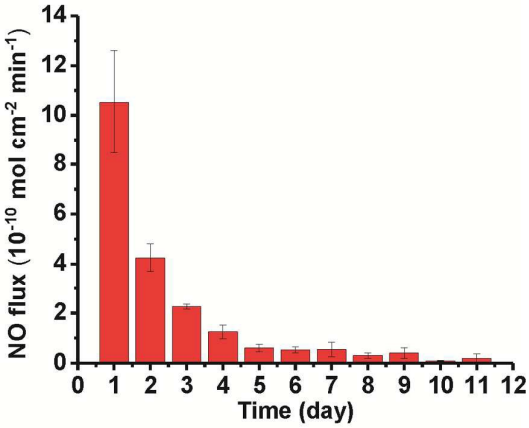

Fig. 7 NO flux for the PDVF tubing incorporated with C_2F_5-SNAP under physiological conditions (PBS with 100 μM EDTA at 37 °C in the dark).

Nitric oxide is well-known to inhibit platelet activation and prevent bacterial proliferation/adhesion. Therefore, NO-release materials have been already well established/documented as a promising platform for developing antithrombotic and antimicrobial materials that can improve the biocompatibility of devices for biomedical applications.[38, 50] Once NO is released from biomaterials *via* doping or grafting the appropriate NO donors (e.g., from catheters), the improved biocompatibility of various polymeric materials is always observed *in vivo* (in animal studies). This has been reported in many previously published animal studies using various polymeric materials including Elast-eon E2As,[52, 60, 68] CarboSil,[54, 67, 74] silicone rubber,[57, 63] and Tygon[59, 61] and so on. Based on the antithrombotic/antiplatelet properties reported previously in the literature for NO release polymers, we can anticipate that our new NO-releasing PVDF tubing will demonstrate

View Article Online
DOI: 10.1039/C8TB01814F

similar antithrombotic properties for at least 7 days, since the NO flux released from the new C_2F_5-SNAP doped PVDF tubing over the first days is > 0.5 x 10^{-10} mol/cm^{2}min.

Cumulative leaching test

The leaching problem remains a challenge for the application of NO donor-doped polymers since the NO donors employed are typically not covalently bonded with the matrix polymers. Leaching of NO donors from the polymer can greatly decrease the efficacy of the NO-releasing flux number and longevity of NO release. Further, the loss of NO donors to the bathing medium raises a concern about toxicity, since an excess amount of NO donor could be rapidly consumed by the local oxyhemoglobin (oxyHb) within blood *via* the rapid reaction of NO with oxyHb. In addition, the leaching of byproducts such as free thiols and disulfides derived from NO donor decomposition can also create potentially toxic species. Therefore, chemical leaching of the initial C_2F_5-SNAP species and potential products (C_2F_5-NAP and its disulfide etc.) from the PDVF tubing was examined. Throughout the measurement of the NO-release process, the concentrations of C_2F_5-NAP, C_2F_5-NAP disulfide and C_2F_5-SNAP were monitored by HPLC-MS daily. Calibration curves of C_2F_5-NAP and C_2F_5-NAP disulfide with the HPLC-MS instrument were established using standard solutions using the corresponding pure chemicals (see Fig. 4S). The leaching of C_2F_5-NAP disulfide was found to be ~ 0.6 nmol per mg of PVDF tubing on the first day (see Fig. 8a). After 9 d of soaking, the total C_2F_5-NAP disulfide doubled (~ 1.2 nmol/mg, 6% of loading of C_2F_5-SNAP in PVDF tubing). C_2F_5-NAP was also detected in the soaking solution with an initial concentration of 1.1 nmol per mg of PVDF tubing (see Fig. 8b). After being stored in soaking solution for 9 d, the leaching of C_2F_5-NAP increased to 1.39 nmol/mg (3% of the total loaded C_2F_5-SNAP in the PVDF tubing). The detection of free thiols in the leaching experiment from NO donor-doped polymer is quite common, and possibly resulted from the reduction of disulfide or hydrolysis of *S*-nitrosothiols.[54] In addition, a small amount of C_2F_5-SNAP (~ 0.1 nmol/mg) was observed on the first day, which was < 1% of the total loading of C_2F_5-SNAP in PVDF tubing. A trace amount of C_2F_5-SNAP was detectable on the second day; however, the C_2F_5-SNAP NO donor was not detected on third day of the HPLC-MS results. In comparison with the chemicals leaching observed from SNAP doped CarboSil, E5-325, and silicone rubber over the first 10 days,[54] the corresponding concentrations of chemical leaching from C_2F_5-SNAP doped PVDF tubing is dramatically less. It is likely the fluorous-fluorous interactions present in the fluorinated materials could be responsible for these low leaching rates.[79-82] More importantly, the absence of C_2F_5-SNAP within the leaching test solution on the third day and the very low leaching of C_2F_5-SNAP (< 1%) indicate that the NO-release from C_2F_5-SNAP doped PVDF tubing mainly comes from C_2F_5-SNAP species within the polymer phase, rather than any donor species that leached out into the soaking solution. The total leaching of chemicals (C_2F_5-SNAP, C_2F_5-NAP, and C_2F_5-NAP disulfide) was < 10% of the initial amount of C_2F_5-SNAP originally present after 11 d.

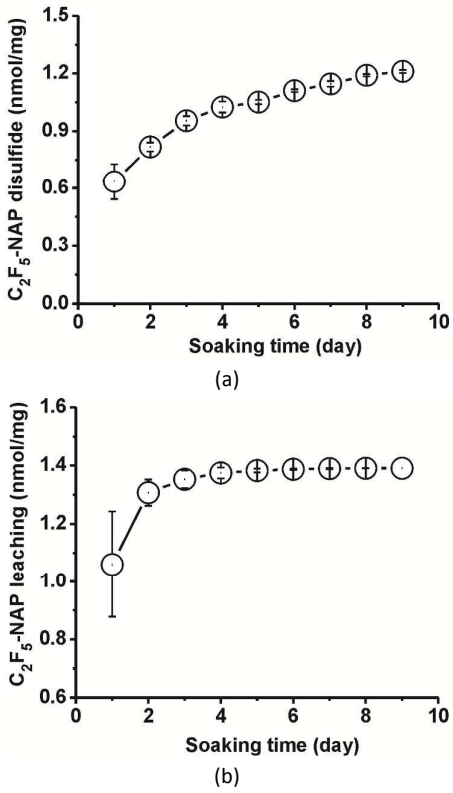

Fig. 8 Cumulative leaching of C_2F_5-NAP disulfide (a) and C_2F_5-NAP (b) into PBS soaking solution (2.0 mL) from the PDVF tubing incorporated with C_2F_5-SNAP at 37 ^{o}C in the dark.

Antimicrobial and anti-biofilm studies

NO-releasing polymers are primarily applied as biomaterials for medical devices.[38, 46] The antimicrobial property derived from surface released NO plays a significant role in the prevention of surface-related infection. Biofilm formation on device surfaces can greatly decrease antibiotic efficiency and opsonophagocytic activity, further leading to chronic infections or inflammations.[89] Therefore, it is of interest to test the antimicrobial and anti-biofilm behavior of the new C_2F_5-SNAP doped PDVF tubing. Since the doped amount can be estimated according to the total NO gas released, using a higher concentration (~ 634.0 mg/mL in THF) of C_2F_5-SNAP in the swelling process will lead to a higher total loading of C_2F_5-SNAP in the PVDF tubing (~ 42.3 nmol/mg), compared to ~ 32.3 nmol/mg achieved when swelling in a lower concentration of C_2F_5-SNAP (400.5 mg/mL in THF). Thus, a higher concentration of C_2F_5-SNAP used in that process will also result in a longer NO release time and a higher loading of C_2F_5-SNAP. In our previous studies, the antimicrobial activity of NO toward *P. aeruginosa* was reported even when the NO flux number from a polymer surface is < 0.5 x 10^{-10} mol/cm^{2}min.[90] In addition, with a higher NO flux rate, enhanced antimicrobial properties are always observed.[90] Therefore, we anticipate that the C_2F_5-SNAP-doped PVDF tubing (~ 42.3 nmol/mg) will exhibit better antimicrobial properties than the one with a total loading of ~ 32.3 nmol/mg, since the total corresponding NO release amount is higher. Therefore, in the

View Article Online
DOI: 10.1039/C8TB01814F

following antimicrobial and antibiofilm studies, the C_2F_5-SNAP-doped PVDF tubing with the higher impregnated amount of C_2F_5-SNAP (~ 42.3 nmol/mg) were used.

Tests were conducted with both gram positive and negative bacterial strains (*S. aureus* and *P. aeruginosa*, respectively). All antimicrobial and anti-biofilm studies were carried out in a CDC biofilm reactor as previously described.[53, 54] Both control and NO-releasing PVDF tubes (labeled as PVDF-NO) were suspended and incubated in a flowing media with each bacterial strain for 7 d at 37 ^{o}C. After 7 days of incubation, the greenish color was still observed in all NO-release tubes, indicating that a significant amount of C_2F_5-SNAP was still present within the PVDF tubing. The results of adhered viable cells for *S. aureus* and *P. aeruginosa* are presented in Figures 9a and 9b. After one week, the NO-release tubing showed significant inhibition for both bacterial strains. In the test against *S. aureus*, the NO-release tubing had > 1 order of magnitude less bacterial counts than that of the control group. A greater effect for the prevention of *P. aeruginosa* was observed, with > two orders of magnitude difference in comparison with the control tubing segments.

Our prior research has reported that a 5-log reduction of the total viable *S. aureus* cells was observed when the NO release was > 0.5 x 10^{-10} mol/cm^{2}min flux during 7 days of release from SNAP impregnated polymers.[54] In addition, > 2-log reduction of *P. aeruginosa* was observed in only 3 h when the NO was 0.5 x 10^{-10} mol/cm^{2}min flux.[90] These literature results indicate that NO release demonstrates significant antimicrobial properties when the flux is ≥ 0.5 x 10^{-10} mol/cm^{2}min. The NO release data shown in Fig. 7 illustrates that the NO flux for the C_2F_5-SNAP doped PVDF tubing is > 0.5 x 10^{-10} mol/cm^{2}min during first 7 days of soaking. From our cumulative leaching test studies, we found that leaching of the C_2F_5-SNAP NO donor is very small, less than 1% of total originally present in the polymer tubing. Further, the total leaching of C_2F_5-NAP disulfide and C_2F_5-NAP species is only 1.2 nmol/mg (6%) and 1.39 nmol/mg (3%) after 9 d of soaking, respectively. Hence, due to the very low leaching of all C_2F_5-SNAP species, the measured surface NO release (~ 42.3 nmol/mg) represents > 99% of the C_2F_5-SNAP NO donor originally doped within the PVDF tubing. Hence, it is very likely that the antimicrobial effects must be coming from released NO, not due to any antimicrobial effect of C_2F_5-NAP (without NO on it) or the dimeric species.

Furthermore, the antimicrobial findings were further confirmed by representative fluorescence images of the biofilms. A clear difference in the images are shown in Fig. 9c and 9d, indicating the preventative role of NO release from tubing with regard to *S. aureus* growth. In Fig. 9d, the surface observed is basically the inherent texture of surface rather than any biofilm/bacteria itself. To provide further evidence the less bacterial adhesion, the corresponding image (to the one with normal exposure shown in Fig. 9d) is provided (see Fig. 5S). In fact, there is only one small red spot located above the image center in Fig. 5S, which is consistent with that in Fig. 9d. Therefore, only very few dead bacteria are adhered on the surface of the NO-releasing PVDF tubing. This result also indicates that the NO-release from PVDF tubing can significantly inhibit the growth of any bacteria on this surface. In addition, a significant difference is observed between Fig. 9e and 9f, illustrating the effect on inhibiting *P. aeruginosa* biofilm formation. It should be noted that in comparison to our previous studies with other polymeric biomaterials,[53-55] our control group of PVDF without NO-release also demonstrated bacterial inhibition (compared to what was observed with non-fluorinated tubing) which is consistent with the innate antimicrobial properties of fluorinated polymers reported in literature.[5] However, *via* the addition of surface NO-release, the C_2F_5-SNAP doped PVDF tubing can more effectively reduce risk of bacterial infections.

Interestingly, compared with the enhanced antimicrobial activity of non-fluorinated polymers that have been observed when doping with SNAP or other NO release agents, for our tests against *S. aureus* and *P. aeruginosa*, somewhat lower antimicrobial effects (in terms of total log decrease in bacterial counts) were observed in comparison with the control tubing segments. This is mostly due to the fact that the PVDF tubing itself has enhanced intrinsic antimicrobial activity compared to nonfluorinated polymers.[3] Since the PVDF tubing used in this work already has less cell adhesion to start with, it is less meaningful to compare our antimicrobial results with those of the other types of nonfluorinated polymers tested to date that have been doped with SNAP or other NO release agents.

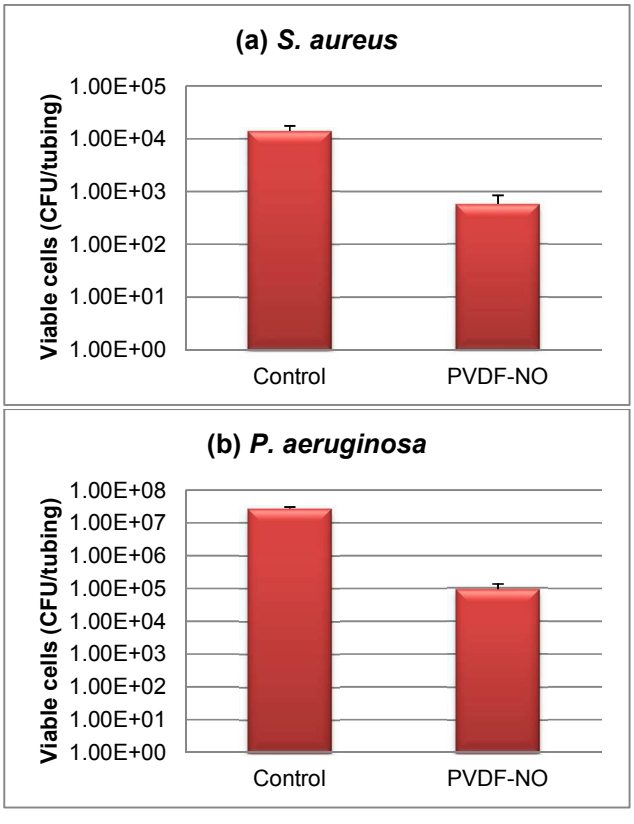

View Article Online
DOI: 10.1039/C8TB01814F

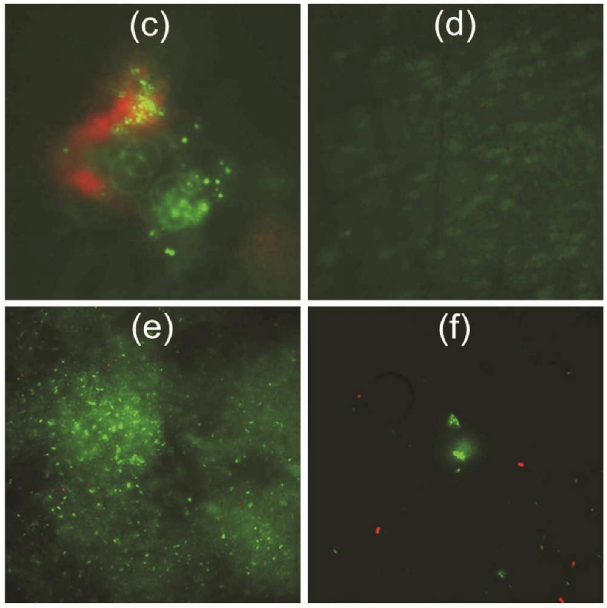

Fig. 9 Antimicrobial and anti-biofilm studies with *S. aureus* and *P. aeruginosa* bacterial strains for 7 d. (a) Plate count number of viable *S. aureus* on the tubing surfaces. (b) Plate count number of viable *P. aeruginosa* on the tubing surfaces. (c) and (d) Representative fluorescence images of the biofilms on the tubing surfaces with *S. aureus* ((c): Control, (d): PVDF-NO). (e) and (f) Representative fluorescence images of the biofilms on the tubing surface with *P. aeruginosa* ((e): Control, (f): PVDF-NO).

Conclusions

In summary, the fluorinated NO donor C_2F_5-SNAP was successfully synthesized, and NO release from a fluoropolymer PVDF impregnated with this new NO donor agent was investigated. C_2F_5-SNAP was found to be thermally unstable due to the presence of its fluorinated functional group. Its corresponding photolytic and thermal decompositions were further characterized in the solution phase. The clean decomposition of C_2F_5-SNAP into NO and C_2F_5-NAP disulfide was demonstrated using a combination of NO determination by NOA and C_2F_5-NAP disulfide analysis by ^{1}H NMR spectroscopy. The PDVF tubing that was swelled in C_2F_5-SNAP solution (~ 634.0 mg/mL in THF) for 24 h showed a loading efficiency of C_2F_5-SNAP ~ 42.3 nmol/mg, which allowed NO release for 11 d under physiological conditions. In the first 7 d, the NO flux number was observed to be greater than that of the physiological level (0.5 flux number). This NO-releasing PVDF tubing demonstrated very low leaching of chemicals including C_2F_5-SNAP, C_2F_5-NAP, and C_2F_5-NAP disulfide, likely resulting from fluorous-fluorous interactions between these fluorinated molecules and PVDF polymer. The low leaching also confirmed that the NO release from C_2F_5-SNAP doped PVDF tubing primarily comes from the surface release of NO from C_2F_5-SNAP within the polymer. Finally, antimicrobial and anti-biofilm studies of C_2F_5-SNAP doped PVDF tubing demonstrated that NO-releasing PVDF can significantly inhibit the growth of both positive and negative *S. aureus* and *P. aeruginosa* bacterial strains after 7 d. These results confirmed the potential for C_2F_5-SNAP doped PVDF tubing to further improve the biocompatibility of fluorinated polymers. To achieve much longer-term NO release purposes, currently, the synthesis of new, relatively stable fluorinated NO donors is underway in our laboratory, which can be further incorporated into fluorinated polymers. Finally, we anticipate that the novel C_2F_5-SNAP doped PVDF composite with NO release capability described here may provide new opportunities to enhance the biocompatibility of biomedical devices for a variety of potential applications.

Experimental section

General materials and methods

All chemicals were directly used without any further purification. The organic reactions were carried out using ACS grade solvent under aerobic conditions. PVDF tubing was purchased from Cole-Parmer company (1/16'' ID × 1/8'' OD, LOT#WQ11443-0002). The synthetic compounds were characterized by ^{1}H and ^{19}F NMR spectroscopy, and high-resolution mass spectrometry (HRMS) with an electrospray ionization source. ^{1}H and ^{19}F NMR spectra were recorded using a Varian 400/500/700 MHz spectrometer. Phosphate-buffered saline (PBS, 10.0 mM, pH 7.40, with 100 μM EDTA) was prepared using NaCl, KCl, Na_2HPO_4 and KH_2PO_4, and the pH of PBS was adjusted by diluted HCl pH solution (referred to a "PBS" throughout).

Synthesis of C_2F_5-NAP and C_2F_5-SNAP

N-Pentafluoropropionylpenicillamine (C_2F_5-NAP) was synthesized by the reaction between *D*-penicillamine and ethyl pentafluoropropionate. To a stirred solution of *D*-penicillamine (3.0120 g, 20.186 mmol) and Et_3N (2.90 mL, d = 0.726 g/mL, 20.8 mmol) in MeOH (250 mL) was added ethyl pentaperfluoropropionate (3.90 mL, d = 1.299 g/mL, 26.4 mmol) dropwise. After stirring for 25 h at room temperature, the solvent was evaporated to dryness and a colorless oil product was obtained. This oil product was then dissolved in water (40 mL) and further acidified with concentrated HCl (37%, 15 mL). After stirring for 15 min, the aqueous solution was extracted with EtOAc (3 × 50 mL). All organic layers were washed with saturated brine (100 mL), dried over Na_2SO_4, and concentrated *in vacuo* to afford a colorless oil as the desired product (5.364 g, 90%). ^{1}H NMR (500 MHz, $CDCl_3$): δ 7.32 (d, *J* = 8.5 Hz, 1H), 4.69 (d, *J* = 9.0 Hz, 1 H), 1.99 (s, 1 H), 1.63 (s, 3 H), 1.41 (s, 3 H). ^{19}F NMR (471 MHz, $CDCl_3$): δ -83.26 (s), -123.74 (d, *J* = 4.71 Hz). HRMS m/z (ESI): calculated for $[M+Na]^+$ 318.0194, found 318.0193.

S-Nitroso-*N*-pentafluoropropionylpenicillamine (C_2F_5-SNAP) was generated from the reaction between C_2F_5-NAP and $NaNO_2$ under acidic conditions. During the reaction process, light exposure was minimized to prevent the decomposition of final target product. HCl (10 mL, 1.0 M) solution was added to a stirred solution of C_2F_5-NAP (1.0135 g, 3.4329 mmol) in MeOH (10 mL) in one portion. Then, a concentrated H_2SO_4 (4.0 mL) solution was added into the reaction mixture. After cooling to room temperature using an ice-water bath, a stock solution of $NaNO_2$ (766.0 mg, 11.10 mmol) dissolved in

View Article Online
DOI: 10.1039/C8TB01814F

water (2 mL) was slowly added dropwise. After stirring for 1 h, the reaction mixture was extracted with CH_2Cl_2 (3 × 50 mL), dried over $NaSO_4$ and concentrated *in vacuo* to afford a greenish oil as target product (1.035 g, 93%). The product was characterized by UV-Vis spectroscopy, $^1H/^{19}F$ NMR spectroscopy and HRMS. UV-Vis: 341 ($n_O \rightarrow \pi^*$) and 595 nm ($n_N \rightarrow \pi^*$). ^1H NMR (700 MHz, DMSO-d_6): δ 10.14 (d, *J* = 9.1 Hz, 1H), 5.33 (d, *J* = 9.1 Hz, 1 H), 2.05 (s, 3 H), 1.98 (s, 3 H). ^{19}F NMR (377 MHz, DMSO-d_6): δ -82.29 (s), -121.22 (d, *J* = 11.31 Hz). HRMS m/z (ESI): calculated for $[M-H]^-$ 323.0130, found 323.0145.

Decomposition kinetic studies of C_2F_5-SNAP and SNAP

The thermal and photo decomposition of the C_2F_5-SNAP and SNAP NO donors under aerobic conditions were monitored by either a PerkinElmer Lambda 35 or a Shimadzu UV-1601 UV-Vis spectrophotometer. The photodecomposition of C_2F_5-SNAP and SNAP was carried out using a Rayonet photochemical reactor (RMR-600) equipped with eight 350 nm lamps (4 W). C_2F_5-SNAP NO donor (~ 206.0 μM) in a mixture of PBS and DMSO (50:50, v/v) was manually scanned by the UV-Vis spectrophotometer at room temperature (23 ^oC) after each irradiation time of 0, 15, 30, 45, 60, 90, 120, 180, 240, 360 and 480 s. The kinetic data was analyzed at 341 nm, by fitting to a first-order rate equation. In a separate thermal decomposition kinetic study at 37 ^oC, C_2F_5-SNAP NO donor (~ 206.0 μM) was dissolved in a mixture of PBS and DMSO (50:50, v/v). The kinetic data was monitored at 341 nm with a time period of 10 min. The resulting kinetic data at 341 nm versus time was fitted into a zero-order rate equation.

Using a similar kinetic method as employed for the C_2F_5-SNAP NO donor, photolysis of SNAP (~ 250.0 μM) in a mixture of PBS and DMSO (50:50, v/v) was manually scanned after each irradiation time of 0, 15, 30, 45, 60, 90, 120, 180, 240, 360, 480 and 780 s. The kinetic data was then analyzed using the absorbance changes at 342 nm with a first-order rate equation. In a thermal decomposition kinetic study of SNAP at 37 ^oC, the SNAP NO donor (~ 206.0 μM) in a mixture of PBS and DMSO (50:50, v/v) was monitored at 342 nm over a time period of 10 min. The resulting absorbance changes at 342 nm versus time was fitted to a zero-order rate equation.

Analysis of decomposition products derived from C_2F_5-SNAP

NO generated from C_2F_5-SNAP NO donor (1.23×10^{-7} mol) was measured using a Sievers 280i chemiluminescence Nitric Oxide Analyzer (NOA). For rapid NO release, the C_2F_5-SNAP NO donor in a mixture of PBS and DMSO (3 mL, 50:50, v/v) was irradiated under a Rayonet photochemical reactor (RMR-600) equipped with eight 350 nm lamps (4 W) at room temperature (23 ^oC). The total moles of NO released from the C_2F_5-SNAP NO donor (1.23×10^{-7} mol) were calculated *via* integration of NO moles detected over time. The C_2F_5-NAP disulfide formed after NO release during thermal decomposition (in the dark) was further characterized by ^1H NMR spectroscopy. For this experiment, a C_2F_5-SNAP NO donor sample in $CDCl_3$ was prepared and characterized by ^1H NMR spectroscopy. This NMR sample was covered with foil and stored in a dark drawer overnight, and was then again characterized by ^1H NMR spectroscopy. After further storage for 4 d in the dark at room temperature, the final spectrum of the resulting sample was measured by ^1H NMR spectroscopy again.

Preparation of C_2F_5-SNAP doped PVDF tubing

C_2F_5-SNAP doped PVDF tubing was prepared using a simple solvent swelling method. Commercially available PVDF tubing (1 inch long , 1/16" ID × 1/8" OD) was swelled in a solution of freshly prepared C_2F_5-SNAP (~ 634.0 mg) dissolved in anhydrous THF (1.0 mL) for 24 h. Then, the swollen PVDF tubing was dried under vacuum for 24 h. This tubing was washed with CH_2Cl_2 (10 times) to completely remove the surface attached chemicals, including any C_2F_5-SNAP and its decomposition products. After being dried under vacuum for another 24 h, the resulting dark green tubing was tested for NO release, chemical leaching, or antimicrobial studies (see below).

Characterization of C_2F_5-SNAP doped PVDF tubing

The NO release profile of C_2F_5-SNAP doped PVDF tubing was recorded by a Sievers 280i chemiluminescence Nitric Oxide Analyzer (NOA). A given piece of C_2F_5-SNAP doped PVDF tubing was loaded onto NOA every day to determine the average NO flux in a solution of PBS (4 mL) at 37 ^oC. Between each measurement, the tubing was soaked in PBS (2 mL), stored in a 37 ^oC oven under dark conditions (within a glass bottle). During the storage process, the bottle's cap had a small hole to release gas pressure built up in the bottle, which was also tightly covered by a parafilm tape to prevent the evaporation of water. The soaking buffer solution obtained on each day was utilized to test for leaching of C_2F_5-SNAP and/or decomposition products. After each measurement of NO release, the tubing was re-soaked in a fresh PBS (2 mL). The leaching test was performed using an Agilent 6520 Accurate-Mass Quadrupole Time-of-Flight (Q-TOF) LC/MS in the electrospray positive-ion mode with a ZORBAX RRHD Eclipse Plus C18 reversed-phase column (2.1 x 50 mm, 1.8 μm). The soaking solution obtained daily from the tubing was used for the determination of C_2F_5-SNAP, C_2F_5-NAP, and C_2F_5-NAP dimer that leached from the C_2F_5-SNAP doped PVDF tubing. In the HPLC method, a gradient was carried out with eluent A (water with 0.1% formic acid) and eluent B (acetonitrile with 0.1% formic acid) from 95% A to 0% A over a 10 min period with a flow rate of 0.4 mL/min. Corresponding calibration curves for pure C_2F_5-NAP and C_2F_5-NAP dimer were obtained to determine their concentrations.

Antimicrobial and anti-biofilm studies

Three pieces of C_2F_5-SNAP doped PVDF tubing (4 cm, 1/16" ID × 1/8" OD) and three pieces of PVDF tubing without the NO donor (4 cm, 1/16" ID × 1/8" OD) were sterilized by 70% ethanol before the antimicrobial and anti-biofilm studies. These pieces of tubing were mounted on the holders of a CDC biofilm reactor (Biosurface Technologies, Bozeman, MT) using rubber bands. The bioreactor was supplemented continuously with 10% LB broth medium at a flow rate of 100 mL/h. The bacteria, *S. aureus*, and *P. aeruginosa* (1% of overnight grown), were inoculated into the bioreactor,

View Article Online
DOI: 10.1039/C8TB01814F

respectively (in separate experiments). The bioreactor was incubated at 37 °C under dark conditions for 7 d. After the pieces of PVDF tubing were removed, and the parts below the rubber bands were divided into two portions, which were used for surface-fluorescence imaging of biofilm formation and for the determination of viable cell counts adhered on the surfaces by using a plate count method. For plate counting, the tubing segment was placed in a centrifuge tube with 2 mL of 10 mM sterilized PBS (pH 7.4) and vortexed to homogenize the biofilm and form a single cell suspension. Then, the solutions were 10-fold serially diluted and plated on LB agar plates for further overnight incubation at 37 °C. To determine the degree of biofilm formation, surface-fluorescence images were taken by fluorescence microscopy (Olympus IX71, Center Valley, PA), after the tubing segments were stained with Live/Death BacLight Bacterial Viability Kit (Life technology, Grand Island, NY). The SYTO-9 green fluorescent dye was analyzed with the excitation light source at 488 nm and emission at 520 nm. Propidium iodide dye was visualized with an excitation light source at 535 nm and emission at 617 nm.

Conflicts of interest

The authors declare no competing financial interest.

Acknowledgements

We gratefully acknowledge the Juvenile Diabetes Research Foundation (JDRF), Grant # 2-SRA-2016-230-Q-R, for supporting this research.

Notes and references

1. M. F. Maitz, *Biosurf. Biotribol.*, 2015, **1**, 161-176.
2. S. Ebnesajjad, in *Expanded PTFE Applications Handbook*, William Andrew Publishing, Oxford, 2017, ch. 9, pp. 193-211.
3. V. Cardoso, D. Correia, C. Ribeiro, M. Fernandes and S. Lanceros-Méndez, *Polymers*, 2018, **10**, 161.
4. A. J. T. Teo, A. Mishra, I. Park, Y.-J. Kim, W.-T. Park and Y.-J. Yoon, *ACS Biomater. Sci. Eng.* , 2016, **2**, 454-472.
5. H. Mori, A. Gupta, S. Torii, E. Harari, H. Jinnouchi, R. Virmani and A. V. Finn, *Expert Rev. Med. Devices*, 2017, **14**, 707-716.
6. H. Teng, *Appl. Sci.*, 2012, **2**, 496.
7. P. C. Nicolson and J. Vogt, *Biomaterials*, 2001, **22**, 3273-3283.
8. T. Koppara, K. Sakakura, E. Pacheco, Q. Cheng, X. Zhao, E. Acampado, A. V. Finn, M. Barakat, L. Maillard, J. Ren, M. Deshpande, F. D. Kolodgie, M. Joner and R. Virmani, *Int. J. Cardiol.*, 2016, **222**, 217-225.
9. T.-Y. Liu, W.-C. Lin, L.-Y. Huang, S.-Y. Chen and M.-C. Yang, *Polym. Adv, Technol.*, 2005, **16**, 413-419.
10. A. M. Garfinkle, A. S. Hoffman, B. D. Ratner, L. O. Reynolds and S. R. Hanson, *ASAIO J.*, 1984, **30**, 432-439.
11. H. Dong Keun, J. Seo Young, K. Young Ha and M. Byoung Goo, *J. Biomater. Sci. Polym. Ed.* , 1992, **3**, 229-241.
12. A. Welle, M. Grunze and D. Tur, *J. Colloid Interface Sci.*, 1998, **197**, 263-274.
13. J.-C. Lin, S.-L. Tiong and C.-Y. Chen, *J. Biomater. Sci. Polym. Ed.* , 2000, **11**, 701-714.
14. L. Pedrini, M. Dondi, A. Magagnoli, F. Magnoni, E. Pisano, E. Del Giudice and M. Santoro, *Ann. Vasc. Surg.* , 2001, **15**, 679-683.
15. A. R. Jahangir, W. G. McClung, R. M. Cornelius, C. B. McCloskey, J. L. Brash and J. P. Santerre, *J. Biomed. Mater. Res.*, 2002, **60**, 135-147.
16. T. M. Massa, W. G. McClung, M. L. Yang, J. Y. C. Ho, J. L. Brash and J. P. Santerre, *J. Biomed. Mater. Res. A*, 2007, **81A**, 178-185.
17. T. Hasebe, S. Yohena, A. Kamijo, Y. Okazaki, A. Hotta, K. Takahashi and T. Suzuki, *J. Biomed. Mater. Res. A*, 2007, **83A**, 1192-1199.
18. X.-W. Wen, S.-P. Pei, H. Li, F. Ai, H. Chen, K.-Y. Li, Q. Wang and Y.-M. Zhang, *J. Mater. Sci.*, 2010, **45**, 2788-2797.
19. D. C. Leslie, A. Waterhouse, J. B. Berthet, T. M. Valentin, A. L. Watters, A. Jain, P. Kim, B. D. Hatton, A. Nedder, K. Donovan, E. H. Super, C. Howell, C. P. Johnson, T. L. Vu, D. E. Bolgen, S. Rifai, A. R. Hansen, M. Aizenberg, M. Super, J. Aizenberg and D. E. Ingber, *Nature Biotechnol.*, 2014, **32**, 1134.
20. K. Tokuda, T. Ogino, M. Kotera and T. Nishino, *Polym. J.*, 2014, **47**, 66.
21. A. Muñoz-Bonilla and M. Fernández-García, *Prog. Polym. Sci.*, 2012, **37**, 281-339.
22. S. Krishnan, R. J. Ward, A. Hexemer, K. E. Sohn, K. L. Lee, E. R. Angert, D. A. Fischer, E. J. Kramer and C. K. Ober, *Langmuir*, 2006, **22**, 11255-11266.
23. E. Martínez-Campos, T. Elzein, A. Bejjani, M. J. García-Granda, A. Santos-Coquillat, V. Ramos, A. Muñoz-Bonilla and J. Rodríguez-Hernández, *ACS Appl. Mater. Interfaces*, 2016, **8**, 6344-6353.
24. J. Lin, X. Chen, C. Chen, J. Hu, C. Zhou, X. Cai, W. Wang, C. Zheng, P. Zhang, J. Cheng, Z. Guo and H. Liu, *ACS Appl. Mater. Interfaces*, 2018, **10**, 6124-6136.
25. H. Ni, T. Jiang, P. Hu, Z. Han, X. Lu and P. Ye, *J. Biomater. Sci. Polym. Ed.* , 2014, **25**, 1920-1945.
26. R. I. Leininger, R. D. Falb and G. A. Grode, *Ann. N. Y. Acad. Sci.* , 1968, **146**, 11-20.
27. M. V. Sefton, A. Sawyer, M. Gorbet, J. P. Black, E. Cheng, C. Gemmell and E. Pottinger-Cooper, *J. Biomed. Mater. Res.*, 2001, **55**, 447-459.
28. S. L. Chin-Quee, S. H. Hsu, K. L. Nguyen-Ehrenreich, J. T. Tai, G. M. Abraham, S. D. Pacetti, Y. F. Chan, G. Nakazawa, F. D. Kolodgie, R. Virmani, N. N. Ding and L. A. Coleman, *Biomaterials*, 2010, **31**, 648-657.
29. M. A. Jamal, K. Garoge, J. S. Rosenblatt, R. Y. Hachem and I. I. Raad, *Antimicrob. Agents Chemother.*, 2015, **59**, 4397-4402.
30. L. Heinemann, J. Walsh and R. Roberts, *J. Diabetes Sci. Technol.* , 2014, **8**, 199-202.
31. L. Heinemann and L. Krinelke, *J. Diabetes Sci. Technol.* , 2012, **6**, 954-964.
32. P. C. Begovac, R. C. Thomson, J. L. Fisher, A. Hughson and A. Gällhagen, *Eur. J. Vasc. Endovasc. Surg.* , 2003, **25**, 432-437.
33. F. He, B. Luo, S. Yuan, B. Liang, C. Choong and S. O. Pehkonen, *RSC Adv.*, 2014, **4**, 105-117.
34. X. Li, X. Hu and T. Cai, *Langmuir*, 2017, **33**, 4477-4489.
35. D. S. Bredt, *Free Radic. Res.*, 1999, **31**, 577-596.
36. H.-T. Chung, H.-O. Pae, B.-M. Choi, T. R. Billiar and Y.-M. Kim, *Biochem. Biophys. Res. Commun.*, 2001, **282**, 1075-1079.
37. N. Toda, K. Ayajiki and T. Okamura, *Pharmacol. Rev.*, 2009, **61**, 62-97.

View Article Online
DOI: 10.1039/C8TB01814F

38. Y. Wo, E. J. Brisbois, R. H. Bartlett and M. E. Meyerhoff, *Biomater. Sci.*, 2016, **4**, 1161-1183.
39. X. Liu, M. J. S. Miller, M. S. Joshi, H. Sadowska-Krowicka, D. A. Clark and J. R. Lancaster, *J. Biol. Chem.*, 1998, **273**, 18709-18713.
40. P. G. Wang, M. Xian, X. Tang, X. Wu, Z. Wen, T. Cai and A. J. Janczuk, *Chem. Rev.*, 2002, **102**, 1091-1134.
41. A. D. Ostrowski and P. C. Ford, *Dalton Trans.*, 2009, 10660-10669.
42. M. R. Miller and I. L. Megson, *Br. J. Pharmacol.*, 2007, **151**, 305-321.
43. T. Munzel and A. Daiber, *Vasc. Pharmacol.*, 2018, **102**, 1-10.
44. W. Fan, B. C. Yung and X. Chen, *Angew. Chem. Int. Ed.*, 2018, **57**, 8383-8394.
45. M. C. Frost, M. M. Reynolds and M. E. Meyerhoff, *Biomaterials*, 2005, **26**, 1685-1693.
46. Z. Sadrearhami, T.-K. Nguyen, R. Namivandi-Zangeneh, K. Jung, E. H. H. Wong and C. Boyer, *J. Mater. Chem. B*, 2018, **6**, 2945-2959.
47. P. Singha, J. Locklin and H. Handa, *Acta Biomater.*, 2017, **50**, 20-40.
48. T. C. Major, H. Handa, G. M. Annich and R. H. Bartlett, *J. Biomater. Appl.*, 2014, **29**, 479-501.
49. E. M. Hetrick and M. H. Schoenfisch, *Chem. Soc. Rev.*, 2006, **35**, 780-789.
50. A. W. Carpenter and M. H. Schoenfisch, *Chem. Soc. Rev.*, 2012, **41**, 3742-3752.
51. W. Cai, J. Wu, C. Xi and M. E. Meyerhoff, *Biomaterials*, 2012, **33**, 7933-7944.
52. E. J. Brisbois, H. Handa, T. C. Major, R. H. Bartlett and M. E. Meyerhoff, *Biomaterials*, 2013, **34**, 6957-6966.
53. A. R. Ketchum, M. P. Kappler, J. Wu, C. Xi and M. E. Meyerhoff, *J. Mater. Chem. B*, 2016, **4**, 422-430.
54. Y. Wo, Z. Li, E. J. Brisbois, A. Colletta, J. Wu, T. C. Major, C. Xi, R. H. Bartlett, A. J. Matzger and M. E. Meyerhoff, *ACS Appl. Mater. Interfaces*, 2015, **7**, 22218-22227.
55. A. Colletta, J. Wu, Y. Wo, M. Kappler, H. Chen, C. Xi and M. E. Meyerhoff, *ACS Biomater. Sci. Eng.*, 2015, **1**, 416-424.
56. H. Ren, J. L. Bull and M. E. Meyerhoff, *ACS Biomater. Sci. Eng.*, 2016, **2**, 1483-1492.
57. Y. Wo, E. J. Brisbois, J. Wu, Z. Li, T. C. Major, A. Mohammed, X. Wang, A. Colletta, J. L. Bull, A. J. Matzger, C. Xi, R. H. Bartlett and M. E. Meyerhoff, *ACS Biomater. Sci. Eng.*, 2017, **3**, 349-359.
58. Y. Wo, L.-C. Xu, Z. Li, A. J. Matzger, M. E. Meyerhoff and C. A. Siedlecki, *Biomater. Sci.*, 2017, **5**, 1265-1278.
59. E. J. Brisbois, M. Kim, X. Wang, A. Mohammed, T. C. Major, J. Wu, J. Brownstein, C. Xi, H. Handa, R. H. Bartlett and M. E. Meyerhoff, *ACS Appl. Mater. Interfaces*, 2016, **8**, 29270-29279.
60. E. J. Brisbois, R. P. Davis, A. M. Jones, T. C. Major, R. H. Bartlett, M. E. Meyerhoff and H. Handa, *J. Mater. Chem. B*, 2015, **3**, 1639-1645.
61. T. C. Major, H. Handa, E. J. Brisbois, M. M. Reynolds, G. M. Annich, M. E. Meyerhoff and R. H. Bartlett, *Biomaterials*, 2013, **34**, 8086-8096.
62. M. J. Goudie, J. Pant and H. Handa, *Sci. Rep.*, 2017, **7**, 13623.
63. E. J. Brisbois, T. C. Major, M. J. Goudie, R. H. Bartlett, M. E. Meyerhoff and H. Handa, *Acta Biomater.*, 2016, **37**, 111-119.
64. P. Singha, J. Pant, M. J. Goudie, C. D. Workman and H. Handa, *Biomater. Sci.*, 2017, **5**, 1246-1255.
65. J. Pant, J. Gao, M. J. Goudie, S. P. Hopkins, J. Locklin and H. Handa, *Acta Biomater.*, 2017, **58**, 421-431.
66. Q. Liu, P. Singha, H. Handa and J. Locklin, *Langmuir*, 2017, **33**, 13105-13113.
67. M. J. Goudie, B. M. Brainard, C. W. Schmiedt and H. Handa, *J. Biomed. Mater. Res. A.*, 2017, **105**, 539-546.
68. E. J. Brisbois, T. C. Major, M. J. Goudie, M. E. Meyerhoff, R. H. Bartlett and H. Handa, *Acta Biomater.*, 2016, **44**, 304-312.
69. M. J. Goudie, E. J. Brisbois, J. Pant, A. Thompson, J. A. Potkay and H. Handa, *Int. J. Polym. Mater.*, 2016, **65**, 769-778.
70. M. N. Mann, B. H. Neufeld, M. J. Hawker, A. Pegalajar-Jurado, L. N. Paricio, M. M. Reynolds and E. R. Fisher, *Biointerphases*, 2016, **11**, 031005.
71. J. M. Joslin, S. M. Lantvit and M. M. Reynolds, *ACS Appl. Mater. Interfaces*, 2013, **5**, 9285-9294.
72. A. Lutzke, J. B. Tapia, M. J. Neufeld and M. M. Reynolds, *ACS Appl. Mater. Interfaces*, 2017, **9**, 2104-2113.
73. A. Koh, A. W. Carpenter, D. L. Slomberg and M. H. Schoenfisch, *ACS Appl. Mater. Interfaces*, 2013, **5**, 7956-7964.
74. E. M. Hetrick, H. L. Prichard, B. Klitzman and M. H. Schoenfisch, *Biomaterials*, 2007, **28**, 4571-4580.
75. C. W. McCarthy, J. Goldman and M. C. Frost, *ACS Appl. Mater. Interfaces*, 2016, **8**, 5898-5905.
76. G. Fleming, J. Aveyard, J. Fothergill, F. McBride, R. Raval and R. D'Sa, *Polymers*, 2017, **9**, 601.
77. A. Lowe, W. Deng, D. W. Smith and K. J. Balkus, *Macromolecules*, 2012, **45**, 5894-5900.
78. H. C. Zhao, M. C. Serrano, D. A. Popowich, M. R. Kibbe and G. A. Ameer, *J. Biomed. Mater. Res. A.*, 2010, **93A**, 356-363.
79. R. K. Kobos, J. W. Eveleigh and R. Arentzen, *Trends Biotechnol.* , 1989, **7**, 101-105.
80. D. Chopra and T. N. G. Row, *CrystEngComm*, 2011, **13**, 2175-2186.
81. H. M. Rapp, S. Bacher, A. Ahrens, W. Rapp, B. Kammerer, G. U. Nienhaus and W. Bannwarth, *ChemPlusChem*, 2012, **77**, 1066-1070.
82. H. Omorodion, B. Twamley, J. A. Platts and R. J. Baker, *Cryst. Growth Des.*, 2015, **15**, 2835-2841.
83. A. R. Ketchum, Ph. D. Thesis, The University of Michigan, Michigan, USA, 2016.
84. T. I. Gorbunova, D. N. Bazhin, A. Y. Zapevalov and V. I. Saloutin, *Russ. J. Appl. Chem.*, 2013, **86**, 992-996.
85. L. Field, R. V. Dilts, R. Ravichandran, P. G. Lenhert and G. E. Carnahan, *J. Chem. Soc. Chem. Commun.*, 1978, 249-250.
86. D. L. H. Williams, *Chem. Comm.*, 1996, 1085-1091.
87. D. L. H. Williams, *Acc. Chem. Res.*, 1999, **32**, 869-876.
88. C. Zhang, T. D. Biggs, N. O. Devarie-Baez, S. Shuang, C. Dong and M. Xian, *Chem. Comm.*, 2017, **53**, 11266-11277.
89. C. Cucarella, M. Á. Tormo, E. Knecht, B. Amorena, Í. Lasa, T. J. Foster and J. R. Penadés, *Infect. Immun.*, 2002, **70**, 3180-3186.
90. H. Ren, J. F. Wu, A. Colletta, M. E. Meyerhoff and C. W. Xi, *Front. Microbiol.*, 2016, **7**, 1260.

View Article Online
DOI: 10.1039/C8TB01814F

Synthesis and Characterization of a Fluorinated *S*-Nitrosothiol as the Nitric Oxide Donor for Fluoropolymer-Based Biomedical Device Applications

Yang Zhou,[a] Qi Zhang,[a] Jianfeng Wu,[b] Chuanwu Xi[b] and Mark E. Meyerhoff*[a]

The first nitric oxide (NO) releasing fluorinated polymer was developed *via* incorporating a new fluorinated NO donor into polyvinylidene fluoride tubing.

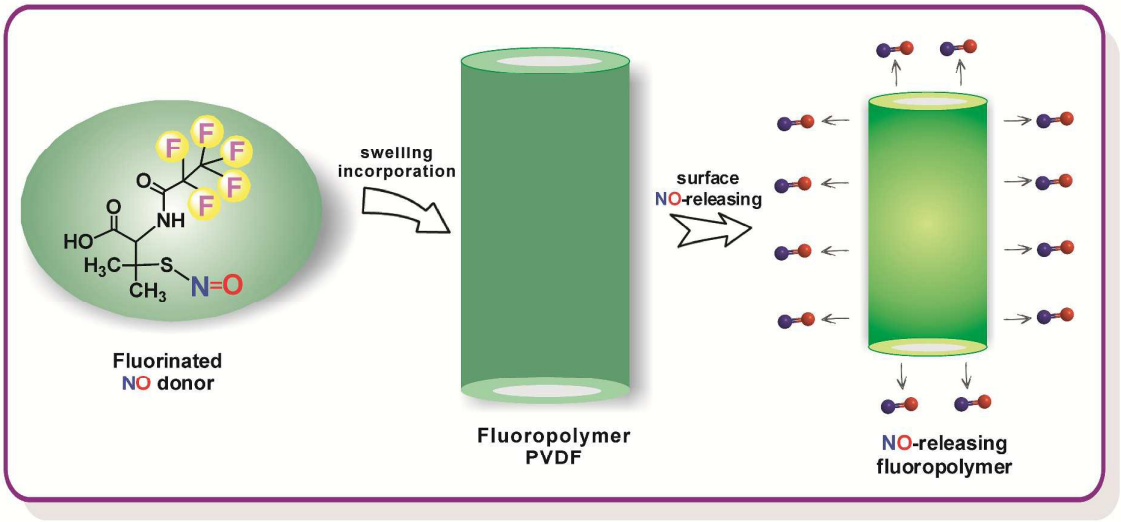

ORCID

Yang Zhou: 0000-0003-0377-4338

Qi Zhang: 0000-0003-2496-8844

Jianfeng Wu: 0000-0002-9770-5538

Chuanwu Xi: 0000-0002-7554-1915

Mark E. Meyerhoff: 0000-0002-7841-281X